ASCOMP
MULTIPHASE FLOW SCIENCE AND TECHNOLOGY

TransAT Report Series

– Presentations –

The C*M*FD code TransAT

Multiphase Flow Modelling

ASCOMP Switzerland

Edited by: Djamel Lakehal

Release date: Sep, 2014

References: TRS-P/ 05-2014

www.ascomp.ch - info@ascomp.ch

Table of Contents

Abstract:
This note describes the suite of multiphase flow models and strategies implemented in the CFD/CMFD code TransAT.

1. Multiphase Flow Modelling

Multiphase flows appear in various industrial processes and in the petroleum industry in particular, where oil, gas and water are often produced and transported together (Hewitt, 2005). During co-current flow in a pipe the multiphase flow topology can acquire a variety of characteristic distributions called flow regimes, or flow patterns, each featuring specific hydrodynamic characteristics (e.g. bubbly, slug, annular, mist, churn) depending on the phasic volumetric flow rates. In addition, the relative volumetric fraction of the phases can change along the pipes either because of heat addition from outside, heat exchanges between the phases or flashing due to depressurization. Some of these hydrodynamic features are clearly undesirable particularly in the hydrocarbon transportation systems, for example slug flow, which may be harmful to some operations components. Such multiphase flows exist in oil and gas pipes to and from the reservoir, too. Indeed, in extraction and injection processes of oil and gas to and from reservoirs, multiphase mixtures of oil, natural gas and water is piped between the reservoir and the surface.

The complexity of multiphase flows in pipes increases with the presence of solid particles, including sand and black powder in gas pipelines. Particle-induced corrosion in oil and gas pipelines made from carbon steel occurs often, which requires the removal of pipe segments affected incurring extra costs and break in the distribution. To this we can add the catalytic reaction between the fluids and the pipe internal walls, including electrochemistry, water chemistry. Black powder deposition may lead to the formation of particle slugs in the pipes that can also be harmful to the operations. Further complexities may appear when phase change between the fluids occurs like the formation of hydrates from methane and light components of oil, which could be remedied through the injection of additives like methanol.

TransAT Multiphase has a rich portfolio of models to cope with most of these flows, including accounting for rheology of complex fluids (Non-Newtonian). For instance, if the flow exhibit multiphase dispersed flow or mixtures, use is made of the Eulerian N-Phase model. If now the flow contains sand, use is made of the Euler-Euler Model (EEM). In case the flow features clear distinct interfaces, and then one resorts to Interface Tracking Methods (ITM), including Level Set. Finally, if the flow encompasses solid particles, the Eulerian-Lagrangian formulation should be activated, including the granular formulation for packed systems. A combination of two or more approaches is also possible including separating the fluids with their proper rheology (heavy and light components).

2. Phase Average Concept

Dispersed, mixed multiphase gas-liquid flows, which cannot be explicitly grid-resolved are tackled using phase-average models, for both laminar and turbulent flows. TransAT does not rely on the two-fluid, six-equation model, but rather on the mixture approach, which is computationally cheaper and amenable to advanced physics.

2-1 Phase-Average: The Mixture approach

In the Homogeneous Algebraic Slip model (Mannin & Taivassalo, 1996) applied to gas-liquid systems, transport equations of mixture quantities are solved rather than phase-specific quantities, i.e.:

$$u_m = \sum \frac{\alpha_k \rho_k u_k}{\alpha_k \rho_k} \; ; \;\; \rho_m = \sum \alpha_k \rho_k$$
$$Y_k = \alpha_k \rho_k / \rho_m \; ; u_D = u_G - u_m \qquad (1)$$

This implies that one mixture momentum equation is solved for the entire flow system, reducing the number of equations to be solved in comparison to the two-fluid model:

$$\frac{\partial \rho_m}{\partial t} + \frac{\partial}{\partial x_j}\left(\rho_m u_{m_j}\right) = 0;$$
$$\frac{\partial \rho_G \alpha_G}{\partial t} + \frac{\partial}{\partial x_j}\left(\rho_G \alpha_G (u_{m_j} + u_{D_j})\right) = 0 \qquad (2\text{-}3)$$
$$\frac{\partial}{\partial t}\left(\rho_m u_{m_j}\right) + \frac{\partial}{\partial x_j} \rho_m \left(u_{m_i} u_{m_j} + \frac{Y_G}{Y_L} u_{D_i} u_{D_j} - \prod_{m,ij} \right) = S_m$$

Closure models are required for slip velocity (uD) and associated stresses $\overline{u_{D_i} u_{D_j}}$. The simplest model used for the slip velocity reads (for bubbly flows):

$$u_{D_j} = \frac{2}{9} \frac{\alpha_L R_b^2 (\rho_G - \rho_L)}{\alpha_G \mu_m} Y_L (Y_L - \alpha_L) \frac{\partial p}{\partial x_j} \qquad (4)$$

2-2 Phase-Average: The N-Phase approach

The N-Phase approach is invoked in situations involving more than two phases, e.g. gas-water-oil-hydrate, with the oil phase comprising both light and heavy components. The N-Phase approach could as well be used in the two-fluid flow context. In the Homogeneous Algebraic Slip framework, the above transport equations become:

$$\frac{\partial \rho_G \alpha_G}{\partial t} + \frac{\partial}{\partial x_j}\left(\rho_G \alpha_G (u_{m_j} + u^k{}_{D_j})\right) = 0$$
$$\frac{\partial}{\partial t}\left(\rho_m u_{m_j}\right) + \frac{\partial}{\partial x_j} \rho_m \left(u_{m_i} u_{m_j} + \frac{\rho_m}{Y_L} \sum\nolimits_k Y_k \, \overline{u^D_{k,i} u^D_{k,j}} - \prod_{m,ij} \right) = S_m \qquad (5\text{-}6)$$

2-3 Phase-Average: Population Balance (PBM) & DQMOM

The N-phase model described above needs as an input parameter the droplet size to determine the drag and lift coefficients. This is however an evolving heterogeneous quantity controlled for instance by droplet coalescence and breakup mechanisms. Furthermore in the same computational volume, a wide range of droplet diameters can coexist. To describe more accurately the evolution of the droplets in the system, instead of solving one equation for the water volume fraction, a PBE can be introduced, describing the evolution in time and space of the Bubble Size Distribution (BSD) ***n****(d;x,t)* that represents the number of droplet per unit volume, with size *d* and can be written as

$$\frac{\partial n}{\partial t} + \frac{\partial}{\partial x_j} V_{p,j}(d) n + \frac{\partial}{\partial d} G n = C(n,n) + B(n,n) \qquad (7)$$

In the above equation, Vp denotes the velocity of the dispersed phase (which in this case is given by the algebraic slip model within the N-Phase), G denotes the growth-rate term (null if there is no phase change or mass transfer), and B and C terms represent the collision mechanism describing respectively droplet coalescence and breakup. These phenomena could be described with various kernels.

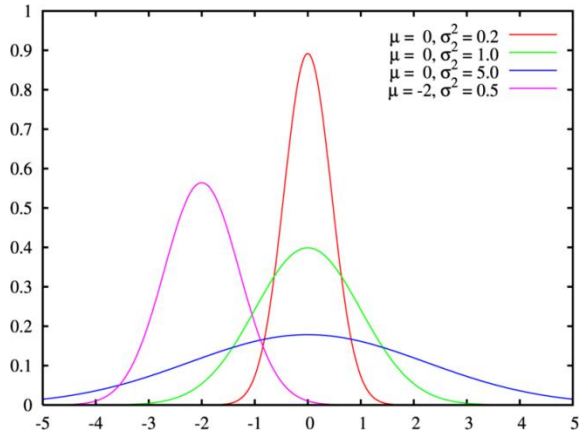

Figure 1: Principles of DQMON: solve for Nodes and Weights to represent the population balance. Y-axis represents the Weights, or how many particles are in that environment); X-axis represents the Nodes, or the values (ξ) of the particles characteristics (e.g. Droplet diameter).

The PBE model is then discretized with the Direct Quadrature Method of Moments (DQMOM, Marchisio and Fox, 2005) consisting in the resolution of transport equations for quadrature nodes and weights (Fig. 1) that approximates exactly the first M moments of the BSD ($\mathbf{m_0}$= n. particles, $\mathbf{m_2}$= interfacial area, $\mathbf{m_3}$ = void fraction, etc.). Each node, corresponding to a particular droplet size and its corresponding weight are transported with their relative velocity (calculated with the N-Phase) and can be considered as a dynamic class with a certain size and a weight that represents the number of droplets per unit volume within that class. This results in higher accuracy and lower computational cost than the standard classes methods. In the test case under study it has been demonstrated that accurate results are already obtained with M=4, tracking exactly up to 3rd order.

In TransAT, we have implemented the following breakage and coalescence kernels:

- bubbly flows: Laakkonen et al. (2007) and Lehr et al. (2002)
- emulsion formation (eg. gravitational separation of oil&water): Grimes et al. (2012), Mitre (2014)
- crystals aggregation: Balakin et al. (2012)
- droplets/bubbles in liquid: Luo (1993), Prince & Blanch (1990), Alopaeus (1999), Coulaloglou et al. (1977)
- other, mechanistic kernels used for solid particles (Marchisio, 2003):
  - aggregation: laminar, brownian, sum, differential, hydrodynamic
  - breakage: powerlaw, exponential, constant
  - fragmentation: symmetric, erosion, massratio, parabolic, uniform

3. Interface Tracking Methods (ITM)

3.1 ITM: The One-Fluid Approach

Interfacial flows refer to multi-phase flow problems that involve two or more immiscible fluids separated by sharp interfaces which evolve in time. Typically, when the fluid on one side of the interface is a gas that exerts shear (tangential) stress upon the interface, the latter is referred to as a free surface. ITM's are best suited for these flows, because they represent the interface topology rather accurately. The single-fluid formalism solves a set of conservation equations with variable material properties and surface forces Lakehal et al. (2002a,b). The incompressible multifluid flow equations within the single-fluid formalism read:

$$\nabla \cdot \boldsymbol{u} = 0 \tag{8}$$

$$\partial_t(\rho \boldsymbol{u}) + \nabla \cdot (\rho \boldsymbol{u}\boldsymbol{u}) = -\nabla p + \nabla \cdot \boldsymbol{\tau} + \boldsymbol{F}_s + \boldsymbol{F}_g \tag{9}$$

where Fg is the gravitational force, Fs is the surface tension force, with **n** standing for the normal vector to the interface. The topology equation describing interfaces is

$$\partial_t C + \boldsymbol{u}.\nabla C = 0 \tag{10}$$

where is the phase function, equal to 0 in the gas phase and 1 in the liquid phase.

3.2 ITM: The Level Set Method

In the Level Set technique (Sussman et al., 1994) the interface between immiscible fluids is represented by a continuous function ϕ, denoting the distance to the interface that is set to zero on the interface, is positive on one side and negative on the other (note that the Heaviside of ϕ is C=0 or 1). Material properties (e.g., density, viscosity, heat capacity, thermal conductivity), body and surface forces are locally updated as a function of ϕ, and smoothed across the interface using a smooth Heaviside function:

$$\rho, \mu = \rho, \mu|_L . H(\phi) + \rho, \mu|_G . [1 - H(\phi)] \tag{11}$$

$$\partial_t \phi + \boldsymbol{u}.\nabla \phi = 0 \tag{12}$$

Further, the fact that ϕ is a continuous function across the interface helps determine the normal vector n to the interface, and thereby the surface curvature $\kappa = -\nabla\phi/|\nabla\phi|$ required for the definition of the surface tension,

$$\mathrm{Fs_i} = \gamma \kappa \mathrm{n_i} \delta^{\mathrm{I}}(\phi) + \nabla_s(\gamma)\delta^{\mathrm{I}}(\phi) \tag{13}$$

in which γ is the surface tension of the fluid and δ^{I} is a smoothed Dirac delta function centered at the interface. The last term in (13) is introduced to model the Marangoni effects related to the change in surface tension coefficient due to temperature or surfactant concentration.

In practice, the level set function ceases to be the signed distance from the interface after a single advection step of Eq. (12). To restore its correct distribution near the interface, a re-distancing equation is adverted to steady state, using 3rd - or 5th order WENO schemes; more details can be found in Lakehal et al. (2002a,b).

3.3 ITM: Large Eddy and Interface Simulation (LEIS)

Turbulent interfacial flows cannot be treated using a statistical turbulence model as the k-ε model for instance, in particular if the interfacial topology deformations are fast compared to the mean flow motion and vigorous. Use is made of LES, which should then be combined with ITM: this is exactly the spirit of LEIS. The filtered LEIS equations were developed by Liovic and Lakehal (2007a,b), and read:

$$\frac{\partial \bar{\rho}}{\partial t} + \nabla.(\boldsymbol{u}\bar{\rho}) = 0 \tag{14}$$

$$\frac{\partial \bar{C}}{\partial t} + \nabla.(\tilde{\boldsymbol{u}}\bar{C}) = 0 \tag{15}$$

$$\frac{\partial \bar{\rho}\tilde{\boldsymbol{u}}}{\partial t} + \nabla.(\bar{\rho}\tilde{\boldsymbol{u}}\tilde{\boldsymbol{u}}) = \nabla.[\bar{\Pi} - \tau] + \bar{\rho}g + \overline{\lambda\kappa\mathbf{n}\delta_2} + E \tag{16}$$

where $\tilde{u}\bar{\rho} \equiv \overline{\rho\boldsymbol{u}}$ at the interface and $\tilde{u} \equiv \bar{\boldsymbol{u}}$ away from it, $\tau \equiv \bar{\rho}(\overline{\boldsymbol{u}\boldsymbol{u}} - \tilde{\boldsymbol{u}}\tilde{\boldsymbol{u}})$ is the SGS stress tensor, E is the sum of the convolution-induced errors that were shown by Liovic and Lakehal (2007b) to be negligible. Away from the interface the filtered mass conservation equation reduces to a pure divergence of the velocity field: $\nabla.\tilde{\boldsymbol{u}} = \nabla.\bar{\boldsymbol{u}} = \mathbf{0}$. The issue concerning the filtered surface tension has also been resolved by the authors cited above: rigorously speaking, the term $\overline{\gamma\kappa\boldsymbol{n}\delta_S}$ can be written as $\overline{\gamma\kappa\boldsymbol{n}\delta_S} = \gamma\bar{\kappa}\bar{\boldsymbol{n}}\delta_S + \varepsilon^{\kappa}$, where the error term should be contained within the last sum term in (16). The SGS modelling within the eddy-viscosity framework makes τ_{ij} proportional to S_{ij}:

$$\tau_{ij} = -2\nu_t S_{ij} + \delta_{ij}\tau_{kk}/3\,; \quad \nu_t = f_\mu^{int}(Cs\Delta)^2\sqrt{2S_{ij}S_{ij}} \tag{17}$$

where the interfacial damping function f_μ^{int} in the vicinity of deformable surfaces is introduced to accommodate the turbulence asymptotic behaviour (Reboux et al., 2006).

4. Lagrangian Particle Tracking (LPT)

4.1 LPT: 1 & 2-way Coupling

The Eulerian-Lagrangian formulation applies to particle-laden (non-resolved flow or component entities) flows, under one-way, two-way or four-way coupling (also known as dense particle flow system). Individual particles are tracked in a Lagrangian way in contrast to the former two approaches, where the flow is solved in a Eulerian way on a fixed grid. One-way coupling refers to particles cloud not affecting the carrier phase, because the field is dilute, in contrast to the two-way coupling, where the flow and turbulence are affected by the presence of particles. The four-way coupling refers to dense particle systems with mild-to-high volume fractions ($\alpha > 5\%$), where the particles interact with each other. In the one- and two-way coupling cases, the carrier phase is solved in an Eulerian way, i.e. mass and momentum equations:

$$\nabla \cdot \boldsymbol{u} = 0 \tag{18}$$

$$\partial_t(\rho\boldsymbol{u}) + \nabla \cdot (\rho\boldsymbol{u}\boldsymbol{u}) = -\nabla p + \nabla \cdot \boldsymbol{\tau} + \boldsymbol{F}_b + \boldsymbol{F}_{fp} \tag{19}$$

combined with the Lagrangian particle equation of motion:

$$\begin{aligned} d_t(v_{p_i}) &= -f_d \frac{9\mu}{2\rho_p d_p^2}\left(u_{p_i} - u_i[x_p(t)]\right) + g \\ f_d &= 1 + 0.15Re_p^{2/3} \end{aligned} \tag{20}$$

where u is the velocity of the carrier phase, u_p is the velocity of the carrier phase at the particle location, v_p is the particle velocity, τ is the viscous stress and π the pressure. Sources terms in (19) denote body forces, F_b, and the rate of momentum exchange per volume between the fluid and particle phases, F_{fp}. The coupling between the fluid and the particles is achieved by projecting the force acting on each particle onto the flow grid:

$$F_{fp} = \sum_{\alpha=1}^{N_p} \frac{\rho_p V_p}{\rho_m V_m} R^{rc} f^{\alpha} W(x^{\alpha}, x^{m}) \quad (21)$$

where α stands for the particle index, N_p for the total number of particles in the flow, f^{α} for the force on a single particle centered at x^{α}, R^{rc} for the ratio between the actual number of particles in the flow and the number of computational particles, and W for the projection weight of the force onto the grid node x_m, which is calculated based on the distance of the particle from those nodes to which the particle force is attributed. V_m is the fluid volume surrounding each grid node, and V_p is the volume of a single particle (Narayanan and Lakehal, 2010).

4.2 LPT: 4-way Coupling, or the Granular Flow Approach

The Eulerian-Lagrangian formulation for dense particle systems featuring mild-to-high volume fractions ($\alpha > 5\%$) in incompressible flow conditions is implemented in TransAT as follows (Eulerian mass and momentum conservation equations for the fluid phase and Lagrangian particle equation of motion):

$$\partial_t(\alpha_f \rho) + \nabla \cdot (\alpha_f \rho \boldsymbol{u}) = 0 \quad (22)$$

$$\partial_t(\alpha_f \rho \boldsymbol{u}) + \nabla \cdot (\alpha_f \rho \boldsymbol{u}\boldsymbol{u}) = -\nabla p + \nabla \cdot \boldsymbol{\tau} + \boldsymbol{F}_b + \boldsymbol{F}_{fp} - \boldsymbol{F}_{coll} \quad (23)$$

where α_f is the volume fraction of fluid ($\alpha_f + \alpha_p = 1$), u is the velocity of the carrier phase, u_p is the velocity of the carrier phase at the particle location, v_p is the particle velocity, Π is the sum of viscous stress σ and pressure p, τ is the turbulent stress tensor (depending whether RANS, V-LES or LES is employed).

In this dense-particle context, the Lagrangian particle equation of motion (23) has an additional source term F_{coll} denoting the inter-particle stress force. The interphase drag model in (23) is set according to Gidaspow (1986). The particle volume fraction is defined from the particle distribution function (ϕ) as

$$\alpha_p = \iiint \phi V_p dV_p d\rho_p du_p \quad (24)$$

The inter-phase momentum transfer function per volume in the fluid momentum equation is

$$F_p = \iiint \phi V_p [A] dV_p d\rho_p du_p; \quad (25)$$

with A standing for the particle acceleration due to aerodynamic drag (1st term in the RHS of Eq. 23), i.e. excluding body forces and inter-particle stress forces (2nd and 3rd terms, respectively). The pressure gradient induced force perceived by the solids is not accounted for. The fluid-independent force F_{coll} is made dependent on the gradient of the so-called inter-particle stress, π, using

$$\boldsymbol{F}_{coll} = \nabla \pi / \rho_p \alpha_p \quad (26)$$

Collisions between particles are estimated by the isotropic part of the inter-particle stress (its off-diagonal elements are neglected.) In most of the models available in the literature π is modelled as a continuum stress (Harris & Crighton, 1994), viz.

$$\boldsymbol{\pi} = \frac{P_s \alpha_p^{\beta(=2-5)}}{max[\alpha_{cp} - \alpha_p; \varepsilon(1-\alpha_p)]} \quad (27)$$

The constant Ps has units of pressure, α_{cp} is the particle volume fraction at close packing, and the constant β is set according to Auzerais et al. (1988). The original expression by Harris & Crighton (1994) was modified to remove the singularity at close pack by adding the expression in the denominator (Snider, 2001); ε is a small number on the order of 10-7. Due to the sharp increase of the collision pressure, near close packing, the collision force acts in a direction so as to push particles away from close packing. In practice the particle volume fraction can locally exceed the close packing limit marginally.

References

G.F. Hewitt, "Three-phase gas-liquid-liquid flows in steady and transients states", Nucl. Eng. Design, 235, 1303-1316, 2005.

M. Mannin, V. Taivassalo, "On the mixture model for multiphase flow", VTT Pubs. 288, 1996.

D.L. Marchisio and R.O. Fox, "Solution of population balance equations using the direct quadrature method of moments", Journal of Aerosol Science, 36:43–73, 2005.

B. Grimes, "Population balance model for batch gravity separation of crude oil and water emulsions. Part I: Model formulation. Journal of Dispersion Science and Technology", 33(4):578–590, 2012.

M. Laakkonen, P. Moilanen, V. Alopaeus, J. Aittamaa, "Modelling local bubble size distributions in agitated vessels", Chem. Eng. Sci., 62, 721-740, 2007.

F. Lehr, D. Mewes, M. Millies, "Bubble-size distribution and flow fields in bubble columns", AIChE J. 42, 1225-1233, 2002.

J. F. Mitre, P. L.C. Lage, M. A. Souza, E. Silva, L. F. Barca, A. O.S. Moraes, R. C.C. Coutinho, E. F. Fonseca, "Droplet breakage and coalescence models for the flow of water-in-oil emulsions through a valve-like element", Chemical Engineering Research and Design, 92, 11, 2493, 2014.

B. Balakin, A.C. Hoffmann, P. Kosinski, "The collision efficiency in a shear flow", Chemical Engineering Science, 2012, 68 (1), 305-312, 2012.

H. Luo, "Coalescence, Breakup and Liquid Circulation in Bubble Column Reactors", PhD thesis from the Norwegian Institute of Technology, Trondheim, Norway 1993.

M.J. Prince and H.W. Blanch, "Bubble Coalescence and Break-up in Air-Sparged Bubble-Columns", Aiche Journal 36 (10):1485-1499, 1990.

C.A. Coulaloglou, L.L. Tavlarides, "Description of interaction processes in agitated liquid-liquid dispersions", Chemical Engineering Science, 32 (11), 1289-1297, 1977.

V. Alopaeus, J. Koskinen, and K. Keskinen, "Simulation of the population balances for liquid-liquid systems in a nonideal stirred tank. Part 1 Description and qualitative validation of the model", Chemical Engineering Science, 54:5887-5899, 1999.

D.L. Marchisio, J.T. Pikturna, R.O. Fox, R.D. Vigil, A.A. Barresi, "Quadrature method of moments for population-balance equations", AIChE Journal 49 (5), 1266-1276, 2003.

D. Lakehal, M. Meier and M. Fulgosi, “Interface tracking for the prediction of interfacial dynamics and mass transfer in multiphase flows". Int. J. Heat & Fluid Flow, 23, 242-255, 2002a.

D. Lakehal, BL Smith, M Milelli, “Large-eddy simulation of bubbly turbulent shear flows”, Journal of Turbulence, Taylor & Francis, 2002b.

M. Sussman, P. Smereka and S. Osher, “A Level set approach for incompressible two-phase flow”, J. Comp. Physics. 114, 146-158, 1994.

P. Liovic, D. Lakehal, “Interface–turbulence interactions in large-scale bubbling processes”, Int. J. Heat and Fluid Flow, Vol. 28, No. 1, p. 127-144, 2007a.

P. Liovic, D. Lakehal, “Multi-Physics Treatment in the Vicinity of Arbitrarily Deformable Fluid-Fluid Interfaces”, J. Comp. Physics, 222, 504-535, 2007b.

S. Reboux, P. Sagaut, D. Lakehal, “Larde-eddy simulation of sheared interfacial flow”, Physics of fluids: a publication of the American Institute of Physics (AIP), Vol. 18, No. 10, p. 105105, 2006.

Narayanan C., Lakehal, D., 4-way coupling in dense particles beds of black powder in pipe flows, FEDSM2010-ICNMM2010-30137, 3rd Joint US-European Fluids Engineering Summer Meeting, August 1-5, 2010, Montreal, Canada.

D. Gidaspow, “Hydrodynamics of fiuidizatlon and heat transfer: Supercomputer modeling”, Applied Mechanics Reviews 39 (1), 1-23, 1986.

F.M. Auzerais, R. Jackson, W.B. Russel, The resolution of shocks and the effects of compressible sediments in transient settling, J. Fluid Mech. 195, 437, 1988

S. E. Harris and D. G. Crighton, “Solutions, solitary waves and voidage disturbances in gas-fluidized beds”, J. Fluid Mech., 266, 243, 1994.

D. M. Snider, An Incompressible Three-Dimensional Multiphase Particle-in-Cell Model for Dense Particle Flows, JCP, 170, 523–549, 2001.